Antiferromagnetic Heisenberg Spin Chain of a Few Cold Atoms
in a One-Dimensional Trap

S. Murmann,[1,*] F. Deuretzbacher,[2,†] G. Zürn,[1] J. Bjerlin,[3] S. M. Reimann,[3] L. Santos,[2] T. Lompe,[1,‡] and S. Jochim[1]

[1]*Physikalisches Institut der Universität Heidelberg, Im Neuenheimer Feld 226, DE-69120 Heidelberg, Germany*
[2]*Institut für Theoretische Physik, Leibniz Universität Hannover, Appelstraße 2, DE-30167 Hannover, Germany*
[3]*Mathematical Physics and NanoLund, LTH, Lund University, SE-22100 Lund, Sweden*

We report on the deterministic preparation of antiferromagnetic Heisenberg spin chains consisting of up to four fermionic atoms in a one-dimensional trap. These chains are stabilized by strong repulsive interactions between the two spin components without the need for an external periodic potential. We independently characterize the spin configuration of the chains by measuring the spin orientation of the outermost particle in the trap and by projecting the spatial wave function of one spin component on single-particle trap levels. Our results are in good agreement with a spin-chain model for fermionized particles and with numerically exact diagonalizations of the full few-fermion system.

The high control and tunability of ultracold atomic systems offer the fascinating possibility to simulate quantum magnetism [1], a topic of fundamental importance in condensed matter physics [2]. Systems of spin-1/2 fermions with antiferromagnetic (AFM) correlations are of particular interest due to the observation of high-temperature superconductivity in cuprates with AFM correlations [3]. The experimental implementation of the necessary exchange couplings is usually realized by superexchange processes of neighboring atoms in the Mott-insulating state of a deep optical lattice. Superexchange couplings were measured in both bosonic [4] and fermionic double-well systems [5] and short-range AFM correlations of fermionic atoms were detected in various lattice geometries [6–8]. Furthermore, superexchange processes were used to study the dynamics of spin impurities above the ferromagnetic (FM) ground state of bosons in the Mott-insulating state of a one-dimensional lattice [9]. Bosonic atoms were also used to simulate AFM Ising spin chains in a tilted optical lattice [10,11]. However, the AFM ground state of spin-1/2 fermions in a deep optical lattice has so far not been realized due to the very low energy scale associated with the superexchange coupling.

This problem can be circumvented in 1D systems, where quantum magnetism can be simulated without an optical lattice [12–14]. In the regime of strong interactions, the spatial wave function of both fermions [15] and bosons [16–18] can be mapped on the wave function of spinless noninteracting fermions [Fig. 1(a)]. In this so-called fermionization limit, the strong interactions lead to the formation of a Wigner-crystal-like state [19–21], which has a highly degenerate ground state when the particles have multiple internal degrees of freedom [Fig. 1(b)] [20–23]. Close to the limit of fermionization, the structure of the quasidegenerate ground-state multiplet [24–33] is determined by an effective Sutherland spin-chain

Hamiltonian, which for two-component systems becomes a Heisenberg model [12,19,21,29,32–34].

In this Letter, we report on the realization of Heisenberg spin chains of $N_\uparrow$ spin-up and $N_\downarrow$ spin-down particles with $(N_\uparrow, N_\downarrow) = (2, 1), (3, 1),$ and $(2, 2)$. We show that under an
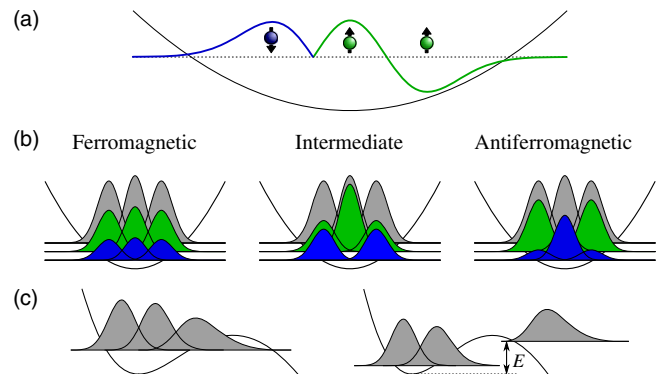

FIG. 1 (color online). Heisenberg spin chain of three fermions. (a) Sketch of two spin-up and one spin-down atom with diverging 1D coupling constant ($g_{1D} = \pm\infty$) in a harmonic trap. If the relative spatial wave function of two distinguishable fermions is symmetric, the strong interactions induce a cusp in the relative wave function of the two particles (left-hand side). This causes them to separate like identical fermions (right-hand side). In this fermionization limit the system forms a Wigner-crystal-like state with fixed ordering of the particles. (b) Single-particle contributions to the total (gray), the spin-up (green), and the spin-down density (blue) of two spin-up and one spin-down atom in the fermionization regime in a harmonic trap. Like in a Wigner crystal, the total densities of the ferromagnetic (left), the intermediate (middle), and the antiferromagnetic state (right) are identical, while their spin densities differ and are determined by a Heisenberg spin-chain Hamiltonian. (c) Densities of three particles before (left) and after (right) the tunneling of one atom with energy E out of a tilted trap. At fermionization, only the rightmost particle can leave the trap in the tunneling process.

adiabatic change of the interaction strength the noninter-acting ground states of these systems evolve into the respective AFM states in the limit of infinitely strong repulsion [24,28]. We identify the AFM states by two independent measurements. First, we use a tunneling technique to measure the spin orientation of the outermost particle of the spin chain. Second, we probe the spatial wave function of the spin-down atom in the (2, 1) and (3, 1) system by projecting it on single-particle trap levels.

In our experiments, we realize a spin-1/2 system by trapping ultracold ^{6}Li atoms in an elongated optical dipole trap [35,39] in their two lowest hyperfine states $|\uparrow\rangle \equiv |j = 1/2, m_j = -1/2; I = 1, m_I = 0\rangle$ and $|\downarrow\rangle \equiv |j = 1/2, m_j = -1/2; I = 1, m_I = 1\rangle$. As the energy of the atoms is much smaller than the lowest transverse excitation energy in the trap, their dynamics are restricted to the longitudinal axis of the trap. In such a quasi-1D system, the interaction strength between ultracold atoms of opposite spin is determined by the 1D coupling constant g_{1D}, which diverges at a confinement-induced resonance (CIR) when the 3D scattering length a_{3D} approaches the harmonic oscillator length of the radial confinement [35,40]. We use a magnetic Feshbach resonance to control a_{3D} and therefore are able to smoothly tune g_{1D} across the CIR. At the same time, scattering between fermionic atoms of the same spin component is forbidden. Throughout this Letter, g_{1D} will be given in units of $a_\parallel \hbar \omega_\parallel$, where $a_\parallel = \sqrt{\hbar/m\omega_\parallel}$ and $\omega_\parallel$ are the harmonic oscillator length and the trap frequency in the longitudinal direction and m is the mass of a ^{6}Li atom.

We start our experiments by preparing a (2, 1), (3, 1), or (2, 2) system in the noninteracting many-particle ground state of the trap [35,39]. By changing the magnetic offset field with a constant rate, we ramp the system into the fermionization regime close to the CIR (Fig. 2), where it forms a spin chain. Below the CIR, g_{1D} is large and positive and the system is in the Tonks regime of strong repulsion [17,18]. When crossing the CIR, g_{1D} changes sign from $+\infty$ to $-\infty$ while the system continuously follows the so-called upper branch [24] into the super-Tonks regime of strong attraction [15,41,42] (Fig. 2). In the super-Tonks regime, the system is in an excited state, which is metastable against decay into bound states.

In a first set of measurements, we identify the states of the spin chains by probing the spin distributions in the trap. Here, we make use of the fact that in the fermionization regime the atoms become impenetrable and therefore their ordering along the longitudinal axis of the trap is fixed. This allows us to determine the spin orientation of the outermost particle in the trap in a tunneling measurement. To do this, we tilt the trap as shown in Fig. 1(c) and thereby allow atoms to tunnel out of the trap. We carefully adjust the trap parameters during the tunneling process, to let exactly one atom [for the (2, 1) and the (3, 1) systems] or two atoms [for the (2, 2) system] tunnel [35]. Finally, we measure the number of spin-up atoms in the final state to determine the spin of the atoms that left the trap during the tunneling process [35]. We define spin-down tunneling as the process in which all spin-down atoms tunnel
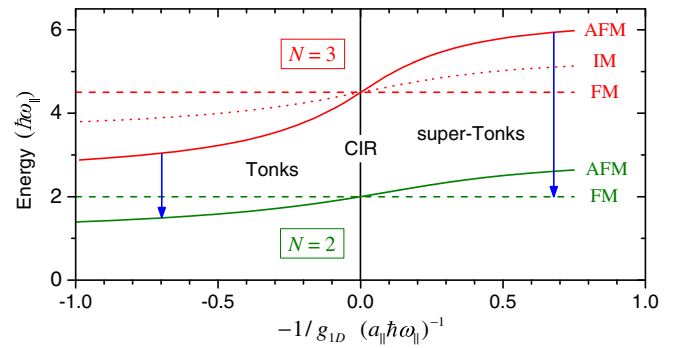

FIG. 2 (color online).   Energies in spin-chain regime. Eigen-energies of two (green) and three (red) strongly interacting spin-1/2 fermions in a 1D harmonic trap as a function of the interaction strength. In the Tonks regime, the antiferromagnetic states are the ground states of each multiplet, while the ferro-magnetic states have the highest energies. In the super-Tonks regime, the ordering of the energy levels is inverted. Close to the confinement-induced resonance (CIR), the energy shifts are linear in $-1/g_{1D}$ and can be determined by a Heisenberg spin-chain Hamiltonian. The system is initially prepared in the noninteracting ground state of the three-particle system at $-1/g_{1D} = -\infty$, which evolves, for increasing $-1/g_{1D}$, into the antiferromagnetic state around the CIR (red solid line). During a ramp across the CIR, the system stays in the antiferromagnetic state, since all eigenstates of the system are decoupled. The blue arrows indicate the predominant channels for the tunneling of one atom below (left) and above (right) the fermionization regime.

out. By repeating this measurement at different magnetic offset fields, we deduce the probability of spin-down tunneling, $P_\downarrow(-1/g_{1D})$, as a function of the inverse 1D coupling constant, as shown in Fig. 3.

As shown in Fig. 1(b) for a (2, 1) system in a harmonic trap, the different states of the spin chain can be uniquely identified by their spin densities [12], specifically by the probability of the outermost spin to point downwards. Since in the fermionization regime the ordering of the atoms in the trap is fixed, only the outermost atom can escape during the tunneling process. Exactly at the CIR, the probability of spin-down tunneling should therefore directly reveal the state of the spin chain [12,29,33]. Away from resonance, the probability of spin-down tunneling is also influenced by the energy of the final in-trap states, favoring final states with lower energy, as indicated by the blue arrows in Fig. 2. To identify the spin states throughout the entire spin-chain regime, we compare our data to the results of a tunneling model, which in the following section is explained for a (2, 1) system.

In our tunneling model, the initial states are eigenstates of a Heisenberg spin-chain Hamiltonian [35], where the exchange couplings J_i between neighboring spins depend on the trap geometry and on the inverse 1D coupling constant [12]. For the (2, 1) system with repulsive interactions and a symmetric trap ($J_1 = J_2 > 0$), these eigenstates are the AFM ground state, the intermediate (IM) state, and the FM state, as shown in Fig. 1(b). During the tunneling process the trap is tilted as shown in Fig. 1(c) and therefore the density
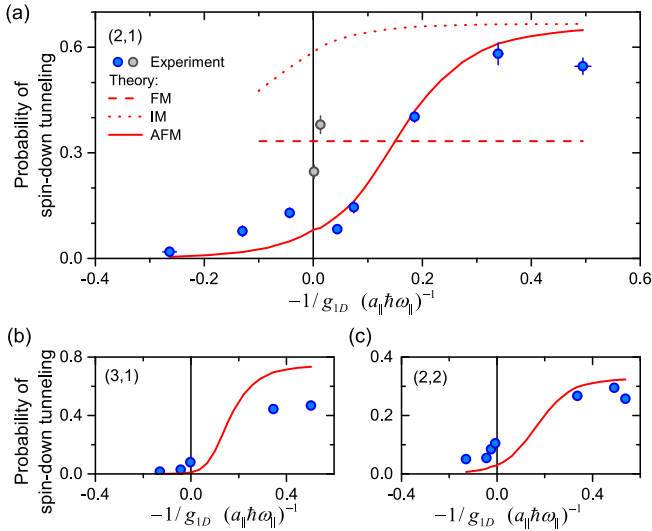
FIG. 3 (color online). Probing the spin distribution. Tunneling probabilities of the spin-down atom in a (2, 1) system (a) and a (3, 1) system (b) and tunneling probability of both spin-down atoms in a (2, 2) system (c) as a function of the interaction strength. The red lines are the solutions of a tunneling model for the antiferromagnetic (solid), the ferromagnetic (dashed), and the intermediate state (dotted). The gray points in (a) indicate a narrow resonance between the antiferromagnetic and the intermediate state of the (2, 1) system close to $-1/g_{1D} = 0$. Error bars denote the 1σ statistical uncertainties.

is not symmetric. Hence, the exchange couplings are not identical anymore ($|J_1| > |J_2|$), which leads to a coherent mixing of the AFM and IM state during the tunneling process [35]. We calculate a probability of approximately 8% for the rightmost spin of the AFM state in the tilted trap to point downwards. This is in good agreement with the blue data points in Fig. 3(a) that cross the CIR at $P_\downarrow \approx 10\%$.

Away from the CIR, the eigenstates of both the three-particle and the two-particle spin chains are nondegenerate (Fig. 2). In this case, the energies of the initial three-particle state $|i\rangle$ and the final two-particle state $|f\rangle$ involved in the tunneling process are important, since their difference determines the energy E of the tunneling particle. The tunneling rate of the particle that leaves the trap is strongly affected by its energy and can be calculated as

$$T_{i,f} \propto |\langle i|f,t\rangle|^2 E e^{-2\gamma(E)}, \tag{1}$$

where $|f,t\rangle = |f\rangle \otimes |t\rangle$ with $|t\rangle$ indicating the spin orientation of the tunneling particle. The tunneling parameter γ is determined by means of a WKB calculation [35]. The probability to tunnel from state $|i\rangle$ to state $|f\rangle$ is given by

$$P_{i,f} = \frac{T_{i,f}}{(\sum_{f'} T_{i,f'})}, \tag{2}$$

where the sum is over all possible final states $|f'\rangle$.

Using Eq. (2), we calculate the probabilities $P_{i,|\uparrow,\uparrow\rangle}$ of tunneling into the spin-polarized final state [red lines in Fig. 3(a)], which is equivalent to the probability of

spin-down tunneling ($P_\downarrow$). Far below the CIR, the energy dependent term $E e^{-2\gamma}$ dominates the outcome of the tunneling rates [Eq. (1)]. Therefore, tunneling into the AFM two-particle ground state $(|\uparrow,\downarrow\rangle - |\downarrow,\uparrow\rangle)/\sqrt{2}$ is strongly favored if its spin overlap to the initial state is not zero. This leads to a limiting value of $P_\downarrow = 0$ for initial AFM and IM states. Above the resonance, the energy ordering of the two-particle FM and AFM states is reversed and tunneling into the FM states is predominant (Fig. 2) [43]. Here, $P_\downarrow$ is determined by the ratio of the spin overlaps between the first two spins of the initial states and the FM two-particle states $|\uparrow,\uparrow\rangle$ and $(|\uparrow,\downarrow\rangle + |\downarrow,\uparrow\rangle)/\sqrt{2}$.

The comparison of the theoretically predicted $P_\downarrow$ of the AFM state in the tilted trap [red solid line in Fig 3(a)] with the experimental data (blue points) shows good agreement, while the FM (red dashed line) and IM (red dotted line) states are clearly excluded. We therefore conclude that before tunneling both below and above the CIR the system is in the AFM state. The gray points at $-1/g_{1D} \approx 0$ indicate a narrow resonance effect that couples the AFM state to the IM state of the spin chain. Since this resonance is accompanied by strongly enhanced three-body losses [35], we suspect it to be caused by a coupling of the AFM and the IM states via a molecular state with center-of-mass excitation. The coupling to such molecular states is strongly enhanced by the anharmonicity of our tilted trap [44].

For the AFM state of the (3, 1) system, a similar calculation predicts $P_\downarrow \approx 1\%$ on resonance and a saturation value of $P_\downarrow \approx 75\%$ deep in the super-Tonks regime [35]. As shown in Fig 3(b), the general trend of our measurements agrees with this prediction for the AFM state, but in the super-Tonks regime, there is a significant deviation. The reason for this deviation is that the calculation assumes an adiabatic lowering of the potential barrier. As a result, the tunneling energies of all tunneling channels are always well below the barrier maximum. We believe that this condition is not fulfilled for the (3, 1) system in the super-Tonks regime, where an especially low potential barrier was used for the tunneling measurement. Indeed, if we model a nonadiabatic lowering of the potential barrier, the contribution from tunneling into the IM state reduces $P_\downarrow$ to values that are compatible with the experimental results [35]. In order to study the spin configuration of the balanced (2, 2) system, we adapt the previous procedure and let two atoms tunnel out of the trap. Here, $P_\downarrow$ is defined as the probability to end up in state $|\uparrow,\uparrow\rangle$, where both spin-down atoms tunneled out of the trap. Again, the predicted $P_\downarrow \approx 4\%$ on resonance and the limiting value of $P_\downarrow \approx 33.3\%$ in the super-Tonks regime are in good agreement with the experiment, as shown in Fig. 3(c).

To independently confirm the results of our measurement of the spin distribution, we perform a second set of measurements that directly probes the spatial wave function of the system. As shown in Fig. 1(a), the relative spatial wave function between identical spins always exhibits a smooth zero crossing, while between distinguishable spins with strong interactions it can exhibit a cusp. The cusps lead to occupancies of high-energy trap levels, while the zero

crossings require only the occupation of the lowest trap levels. In general, the more symmetric the spatial wave function of a state is, the more cusps it will contain. Therefore, the occupation-number distribution on single-particle trap levels directly reveals the spin configuration of the system.

To probe this distribution, we prepare an interacting (2, 1) or (3, 1) system and remove all atoms of the spin-up component from the trap with a short pulse of light. The light is σ^- polarized and resonant to the D_2 transition of the spin-up atoms ($|\uparrow\rangle = |j=1/2, m_j=-1/2; I=1, m_I=0\rangle$ to $|j=3/2, m_j=-3/2; I=1, m_I=0\rangle$). We confirm that within our experimental fidelity all spin-up atoms are removed from the trap by the light pulse, while only 3% of the population of spin-down atoms is lost. With 15 μs the duration of the light pulse is significantly shorter than the inverse longitudinal trap frequency of approximately 100 μs, which sets the time scale of redistribution along the spin chain. This process therefore projects the spin-down component of the wave function of the interacting $(N_\uparrow, 1)$-particle system on single-particle trap levels. Finally, we measure the mean occupancies on the single-particle trap levels [35]. In Fig. 4 we compare the mean occupancies of the spin-down atom for the (2, 1) and the (3, 1) systems in the super-Tonks regime with the theoretical prediction that we obtained by numerically diagonalizing the many-body Hamiltonian for these systems. The comparison shows that both systems are in the AFM spin state and thereby confirms that our systems follow this state throughout the fermionization regime.

In conclusion, we have prepared antiferromagnetic Heisenberg spin chains of up to four atoms in a one-dimensional trap and independently probed the spin distributions and spatial wave functions of the systems. This constitutes a direct observation of quantum magnetism beyond two-particle correlations in a system of ultracold fermionic atoms. By using the methods developed in Ref. [5], multiple spin chains can be realized and coupled, which offers a new approach to studying two- and three-dimensional quantum magnetism.
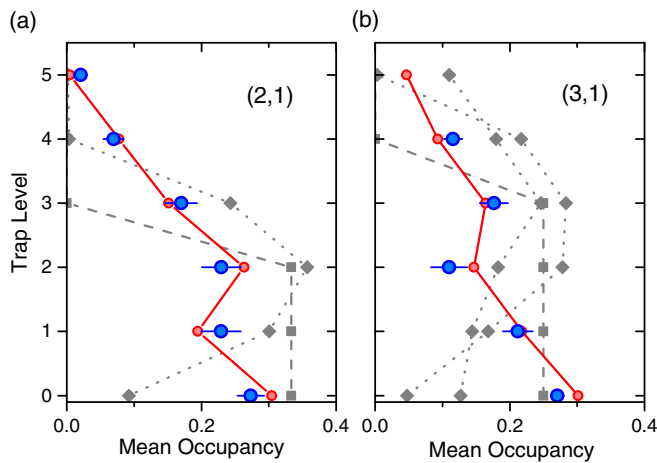
FIG. 4 (color online). Probing the spatial wave function. Occupation-number distribution of the spin-down atom on single-particle trap levels for an initial (a) (2, 1) and (b) (3, 1) system. The red and gray symbols show theoretical predictions for the antiferromagnetic state (red circles), the ferromagnetic state (gray squares), and intermediate states (gray diamonds). Both measurements (blue points) were made in the super-Tonks regime $[-1/g_{1D} = 0.586 \pm 0.014$ for the (2, 1) system and $-1/g_{1D} = 0.536 \pm 0.013$ for the (3, 1) system] to show that both systems stay in the respective antiferromagnetic states throughout the regime of fermionization. Error bars denote the 1σ statistical uncertainty.

*murmann@physi.uni-heidelberg.de
†frank.deuretzbacher@itp.uni-hannover.de
‡Present address: Institut für Laserphysik, Universität Hamburg, Luruper Chaussee 149, DE-22761 Hamburg, Germany.

[1] M. Lewenstein, A. Sanpera, V. Ahufinger, B. Damski, A. Sen De, and U. Sen, Ultracold atomic gases in optical lattices: Mimicking condensed matter physics and beyond, Adv. Phys. **56**, 243 (2007).

[2] A. Auerbach, *Interacting Electrons and Quantum Magnetism* (Springer, New York, 1994).

[3] M. R. Norman, The challenge of unconventional superconductivity, Science **332**, 196 (2011).

[4] S. Trotzky, P. Cheinet, S. Fölling, M. Feld, U. Schnorrberger, A. M. Rey, A. Polkovnikov, E. A. Demler, M. D. Lukin, and I. Bloch, Time-resolved observation and control of superexchange interactions with ultracold atoms in optical lattices, Science **319**, 295 (2008).

[5] S. Murmann, A. Bergschneider, V. M. Klinkhamer, G. Zürn, T. Lompe, and S. Jochim, Two Fermions in a Double Well: Exploring a Fundamental Building Block of the Hubbard Model, Phys. Rev. Lett. **114**, 080402 (2015).

[6] D. Greif, T. Uehlinger, G. Jotzu, L. Tarruell, and T. Esslinger, Short-range quantum magnetism of ultracold fermions in an optical lattice, Science **340**, 1307 (2013).

[7] R. A. Hart, P. M. Duarte, T.-L. Yang, X. Liu, T. Paiva, E. Khatami, R. T. Scalettar, N. Trivedi, D. A. Huse, and R. G. Hulet, Observation of antiferromagnetic correlations in the Hubbard model with ultracold atoms, Nature (London) **519**, 211 (2015).

[8] M. Messer, R. Desbuquois, T. Uehlinger, G. Jotzu, S. Huber, D. Greif, and T. Esslinger, Exploring Competing Density Order in the Ionic Hubbard Model with Ultracold Fermions, Phys. Rev. Lett. **115**, 115303 (2015).

[9] T. Fukuhara, A. Kantian, M. Endres, M. Cheneau, P. Schauß, S. Hild, D. Bellem, U. Schollwöck, T. Giamarchi,

C. Gross, I. Bloch, and S. Kuhr, Quantum dynamics of a mobile spin impurity, Nat. Phys. **9**, 235 (2013).

[10] J. Simon, W. S. Bakr, R. Ma, M. E. Tai, P. M. Preiss, and M. Greiner, Quantum simulation of antiferromagnetic spin chains in an optical lattice, Nature (London) **472**, 307 (2011).

[11] F. Meinert, M. J. Mark, E. Kirilov, K. Lauber, P. Weinmann, A. J. Daley, and H.-C. Nägerl, Quantum Quench in an Atomic One-Dimensional Ising Chain, Phys. Rev. Lett. **111**, 053003 (2013).

[12] F. Deuretzbacher, D. Becker, J. Bjerlin, S. M. Reimann, and L. Santos, Quantum magnetism without lattices in strongly interacting one-dimensional spinor gases, Phys. Rev. A **90**, 013611 (2014).

[13] M. E. Beverland, G. Alagic, M. J. Martin, A. P. Koller, A. M. Rey, and A. V. Gorshkov, Realizing exactly solvable SU(N) magnets with thermal atoms, arXiv:1409.3234.

[14] G. Pagano, M. Mancini, G. Cappellini, P. Lombardi, F. Schäfer, H. Hu, X.-J. Liu, J. Catani, C. Sias, M. Inguscio, and L. Fallani, A one-dimensional liquid of fermions with tunable spin, Nat. Phys. **10**, 198 (2014).

[15] G. Zürn, F. Serwane, T. Lompe, A. N. Wenz, M. G. Ries, J. E. Bohn, and S. Jochim, Fermionization of Two Distinguishable Fermions, Phys. Rev. Lett. **108**, 075303 (2012).

[16] M. Girardeau, Relationship between systems of impenetrable bosons and fermions in one dimension, J. Math. Phys. (N.Y.) **1**, 516 (1960).

[17] B. Paredes, A. Widera, V. Murg, O. Mandel, S. Fölling, I. Cirac, G. V. Shlyapnikov, T. W. Hänsch, and I. Bloch, Tonks-Girardeau gas of ultracold atoms in an optical lattice, Nature (London) **429**, 277 (2004).

[18] T. Kinoshita, T. Wenger, and D. S. Weiss, Observation of a one-dimensional Tonks-Girardeau gas, Science **305**, 1125 (2004).

[19] K. A. Matveev, Conductance of a Quantum Wire in the Wigner-Crystal Regime, Phys. Rev. Lett. **92**, 106801 (2004); K. A. Matveev, Conductance of a quantum wire at low electron density, Phys. Rev. B **70**, 245319 (2004).

[20] F. Deuretzbacher, K. Fredenhagen, D. Becker, K. Bongs, K. Sengstock, and D. Pfannkuche, Exact Solution of Strongly Interacting Quasi-One-Dimensional Spinor Bose Gases, Phys. Rev. Lett. **100**, 160405 (2008).

[21] K. A. Matveev and A. Furusaki, Spectral Functions of Strongly Interacting Isospin-1/2 Bosons in One Dimension, Phys. Rev. Lett. **101**, 170403 (2008).

[22] M. D. Girardeau and A. Minguzzi, Soluble Models of Strongly Interacting Ultracold Gas Mixtures in Tight Waveguides, Phys. Rev. Lett. **99**, 230402 (2007).

[23] L. Guan, S. Chen, Y. Wang, and Z.-Q. Ma, Exact Solution for Infinitely Strongly Interacting Fermi Gases in Tight Waveguides, Phys. Rev. Lett. **102**, 160402 (2009).

[24] S. E. Gharashi and D. Blume, Correlations of the Upper Branch of 1D Harmonically Trapped Two-Component Fermi Gases, Phys. Rev. Lett. **111**, 045302 (2013).

[25] P. O. Bugnion and G. J. Conduit, Ferromagnetic spin correlations in a few-fermion system, Phys. Rev. A **87**, 060502 (R) (2013).

[26] T. Sowiński, T. Grass, O. Dutta, and M. Lewenstein, Few interacting fermions in one-dimensional harmonic trap, Phys. Rev. A **88**, 033607 (2013).

[27] X. Cui and T.-L. Ho, Ground-state ferromagnetic transition in strongly repulsive one-dimensional Fermi gases, Phys. Rev. A **89**, 023611 (2014).

[28] E. J. Lindgren, J. Rotureau, C. Forssén, A. G. Volosniev, and N. T. Zinner, Fermionization of two-component few-fermion systems in a one-dimensional harmonic trap, New J. Phys. **16**, 063003 (2014).

[29] A. G. Volosniev, D. V. Fedorov, A. S. Jensen, M. Valiente, and N. T. Zinner, Strongly interacting confined quantum systems in one dimension, Nat. Commun. **5**, 5300 (2014).

[30] N. L. Harshman, Spectroscopy for a few atoms harmonically trapped in one dimension, Phys. Rev. A **89**, 033633 (2014).

[31] M. A. García-March, B. Juliá-Díaz, G. E. Astrakharchik, J. Boronat, and A. Polls, Distinguishability, degeneracy, and correlations in three harmonically trapped bosons in one dimension, Phys. Rev. A **90**, 063605 (2014).

[32] L. Yang, L. Guan, and H. Pu, Strongly interacting quantum gases in one-dimensional traps, Phys. Rev. A **91**, 043634 (2015).

[33] J. Levinsen, P. Massignan, G. M. Bruun, and M. M. Parish, Strong-coupling ansatz for the one-dimensional Fermi gas in a harmonic potential, Sci. Adv. **1**, e1500197 (2015).

[34] X.-W. Guan, M. T. Batchelor, and J.-Y. Lee, Magnetic ordering and quantum statistical effects in strongly repulsive Fermi-Fermi and Bose-Fermi mixtures, Phys. Rev. A **78**, 023621 (2008).

[35] See Supplemental Material at http://link.aps.org/supplemental/10.1103/PhysRevLett.115.215301 for details on the experimental methods, the data evaluation, and the theoretical models, which includes Refs. [36–38].

[36] G. Zürn, Ph.D. thesis, University of Heidelberg, 2012.

[37] G. Zürn, T. Lompe, A. N. Wenz, S. Jochim, P. S. Julienne, and J. M. Hutson, Precise Characterization of ^{6}Li Feshbach Resonances Using Trap-Sideband-Resolved RF Spectroscopy of Weakly Bound Molecules, Phys. Rev. Lett. **110**, 135301 (2013).

[38] S. E. Gharashi, X. Y. Yin, Y. Yan, and D. Blume, One-dimensional Fermi gas with a single impurity in a harmonic trap: Perturbative description of the upper branch, Phys. Rev. A **91**, 013620 (2015).

[39] F. Serwane, G. Zürn, T. Lompe, T. B. Ottenstein, A. N. Wenz, and S. Jochim, Deterministic preparation of a tunable few-fermion system, Science **332**, 336 (2011).

[40] M. Olshanii, Atomic Scattering in the Presence of an External Confinement and a Gas of Impenetrable Bosons, Phys. Rev. Lett. **81**, 938 (1998).

[41] G. E. Astrakharchik, J. Boronat, J. Casulleras, and S. Giorgini, Beyond the Tonks-Girardeau Gas: Strongly Correlated Regime in Quasi-One-Dimensional Bose Gases, Phys. Rev. Lett. **95**, 190407 (2005).

[42] E. Haller, M. Gustavsson, M. J. Mark, J. G. Danzl, R. Hart, G. Pupillo, and H.-C. Nägerl, Realization of an excited, strongly correlated quantum gas phase, Science **325**, 1224 (2009).

[43] At the values of g_{1D} attainable in our experiment, the spatial wave function overlap between the spin-chain states and the molecular ground state is negligible. We expect that for a small negative g_{1D} tunneling into the molecular state is predominant.

[44] S. Sala, G. Zürn, T. Lompe, A. N. Wenz, S. Murmann, F. Serwane, S. Jochim, and A. Saenz, Coherent Molecule Formation in Anharmonic Potentials Near Confinement-Induced Resonances, Phys. Rev. Lett. **110**, 203202 (2013).